

Chloride Labilization Resulting from Nucleophilic Addition to *cis*-Ru(tpy)(CO)₂Cl⁺PF₆[−]: Synthesis and Characterization of New CO₂-Bridged and Formate Complexes of Ruthenium

Dorothy H. Gibson,* Bradley A. Sleadd, Mark S. Mashuta, and John F. Richardson

Department of Chemistry and Center for Chemical Catalysis, University of Louisville, Louisville, Kentucky 40292

Received June 11, 1997[®]

Reaction of *cis*-Ru(tpy)(CO)₂Cl⁺PF₆[−] (**1**; tpy = 2,2':6',2''-terpyridyl) with aqueous Na₂CO₃ in acetonitrile yields the CO₂-bridged complex *cis,cis*-(CH₃CN)(CO)(tpy)Ru(CO)₂Ru(tpy)-(CO)₂²⁺2PF₆[−] (**3**). Reaction of **1** with aqueous NaOCHO yields the corresponding η¹-formate complex **4**; reaction of **4** with aqueous Na₂CO₃ also provides **3**. Reaction of **3** with CO results in displacement of acetonitrile and formation of **5**, *cis,cis*-(CO)₂(tpy)Ru(CO)₂Ru(tpy)(CO)₂²⁺2PF₆[−]. Reaction paths leading to **3** and **4** from **1** are thought to occur by base-assisted trans labilization of chloride resulting from conversion of a π-acceptor ligand (CO) to a σ-donor (COOH). Support for proposed steps in the reaction paths leading to **3** and **4** was provided by a trapping experiment in which **1** reacts with *cis*-Ru(bpy)₂(CO)COOH⁺PF₆[−] in the presence of aqueous Na₂CO₃ to give *cis,cis*-(CO)(bpy)₂Ru(CO)₂Ru(tpy)(CO)₂²⁺2PF₆[−] (**7**; bpy = 2,2'-bipyridyl), which has been structurally characterized. Parallels between these reactions and the halide labilizations which occur with ruthenium or rhenium polypyridyl complexes during photochemical or electrochemical reductions of CO₂ are discussed.

Introduction

Ruthenium and rhenium carbonyl halide complexes, especially chlorides and bromides, bearing polypyridyl ligands are effective as photocatalysts and electrocatalysts for the reduction of CO₂.¹ Common to most of the proposed catalytic cycles in these reactions are steps in which halide ion dissociation follows electron transfer to the complexes. Since carbon dioxide complexes have not been observed in these reactions but are usually proposed as intermediates, we have sought to prepare model compounds whose properties might enhance the understanding of steps in the catalytic cycles. We report the characterization of the new complex *cis*-Ru(tpy)(CO)₂Cl⁺PF₆[−] (**1**; tpy = 2,2':6',2''-terpyridyl) and the results of its reactions in the presence of several nucleophiles, including weak aqueous bases.

Results and Discussion

Synthesis of New Compounds. Reaction of [Ru(CO)₂Cl₂]_n² with 2,2':6',2''-terpyridine in refluxing EtOH/H₂O, followed by anion exchange using NH₄PF₆, gave an off-white solid which has been characterized by spectral data and elemental analysis. The ¹H NMR data showed one lower field doublet at δ 8.75 and a series of multiplets between δ 8.49 and 7.67. The ¹³C NMR data showed 8 resonances for 15 carbons in the region between δ 158.08 and 125.29; a mirror plane which bisects the terpyridyl ligand gives rise to internal equivalence of the carbon (and proton) resonances. Terminal carbonyl resonances in the product appear at δ 194.94 and 187.31. DRIFTS data show ν_{CO} signals at 2092 and 2029 cm^{−1}; these data are consistent with the formulation as the dicarbonyl cation *cis*-Ru(tpy)(CO)₂Cl⁺PF₆[−] (**1**). Substitution of the hexafluorophosphate counterion by tetraphenylborate provided a crystalline material, *cis*-Ru(tpy)(CO)₂Cl⁺BPh₄[−] (**1a**), which has been structurally characterized (see discussion below); the spectral properties of the cation portion of **1a** are closely similar to those of **1**.

In previous work, we have successfully employed aqueous Na₂CO₃ as a reagent for the generation of metalcarboxylic acids from metal carbonyl cations.³ In our experience, and that of others,⁴ aqueous Na₂CO₃ is sufficiently basic to provide OH[−] for nucleophilic attack on a carbonyl ligand in a cationic metal complex but not basic enough to deprotonate the resulting metalcarboxylic acid. Reaction of **1** with excess aqueous

[®] Abstract published in *Advance ACS Abstracts*, September 1, 1997.

(1) (a) Hawecker, J.; Lehn, J. M.; Ziessel, R. *J. Chem. Soc., Chem. Commun.* **1983**, 536. (b) Sullivan, B. P.; Bolinger, C. M.; Conrad, D.; Vining, T. J.; Meyer, T. J. *J. Chem. Soc., Chem. Commun.* **1985**, 1414. (c) Sullivan, B. P.; Conrad, D.; Meyer, T. J. *Inorg. Chem.* **1985**, *24*, 3640. (d) Hawecker, J.; Lehn, J.-M.; Ziessel, R. *Helv. Chim. Acta* **1986**, *69*, 1990. (e) Ishida, H.; Tanaka, K.; Tanaka, T. *Organometallics* **1987**, *6*, 181. (f) Bruce, M. R. M.; Megehee, E.; Sullivan, B. P.; Thorp, H.; O'Toole, T. R.; Downard, A.; Meyer, T. J. *Organometallics* **1988**, *7*, 238. (g) Sullivan, B. P.; Bruce, M. R. M.; O'Toole, T. R.; Bolinger, C. M.; Megehee, E.; Thorp, H.; Meyer, T. J. In *Catalytic Activation of Carbon Dioxide*; Ayers, W. M., Ed.; ACS Syms. Ser. 363; American Chemical Society: Washington, D. C., 1988; Chapter 6. (h) Ziessel, R. In *Catalysis by Metal Complexes: Photosensitization and Photocatalysis Using Inorganic and Organometallic Compounds*; Kalyanasundaram, K., Grätzel, M., Eds.; Kluwer Academic: Dordrecht, The Netherlands, 1993 p 217. (i) Christensen, P.; Hammett, A.; Muir, A. V. G.; Timney, J. H. *J. Chem. Soc., Dalton Trans.* **1992**, 1455. (j) Yoshida, T.; Tsutsumida, K.; Teratani, S.; Yasufuku, K.; Kaneko, M. *J. Chem. Soc., Chem. Commun.* **1993**, 631. (k) Stor, G. J.; Hartl, F.; van Outersterp, J. W. M.; Stufkens, D. J. *Organometallics* **1995**, *14*, 115. (l) Johnson, F. P. A.; George, M. W.; Hartl, F.; Turner, J. J. *Organometallics* **1996**, *15*, 3374. (m) Klein, A.; Vogler, C.; Kaim, W. *Organometallics* **1996**, *15*, 236.

(2) Colton, R.; Farthing, R. H. *Aust. J. Chem.* **1967**, *20*, 1283.

(3) Gibson, D. H.; Mehta, J. M.; Ye, M.; Richardson, J. F.; Mashuta, M. S. *Organometallics* **1994**, *13*, 1070.

(4) Suzuki, H.; Omori, H.; Moro-oka, Y. *J. Organomet. Chem.* **1987**, *327*, C49.

Na_2CO_3 did not provide the expected metallocarboxylic acid, however. The reaction afforded a product whose ^1H NMR spectrum showed a series of multiplets between δ 8.49 and 7.17 which are assigned to two sets of terpyridyl protons, each displaying internal equivalence characteristic of compounds having mirror planes which bisect both terpyridyl ligands. The ^{13}C NMR spectrum showed 4 low-field signals at δ 204.25, 198.23, 195.38, and 190.18, which have been assigned to three terminal carbonyls and a carboxylate carbon, and 16 resonances for 30 carbons in the region between δ 157.90 and 122.26, which are assigned to the terpyridyl carbons. DRIFTS data showed ν_{CO} signals at 2069, 2013, and 1953 cm^{-1} and ν_{OCO} bands at 1503 and 1177 cm^{-1} . The ν_{OCO} values for this compound are very similar to those in the related CO_2 -bridged compound *cis,cis*- $\text{Ru}(\text{bpy})_2(\text{CO})(\text{CO}_2)\text{Ru}(\text{bpy})_2(\text{CO})^{2+}2\text{PF}_6^-$ (**2**; bpy = 2,2'-bipyridyl),⁵ which shows ν_{OCO} signals at 1507 and 1176 cm^{-1} , as well as other compounds with $\mu_2\text{-}\eta^2$ -type bridging CO_2 ligands.⁶ Weak bands were also observed for the coordinated nitrile (2313 and 2283 cm^{-1}); these are similar in position, and in intensity, to those reported⁷ for *cis*(CO),*trans*(CH_3CN)- $\text{Ru}(\text{bpy})(\text{CO})_2(\text{CH}_3\text{CN})^{2+}2\text{PF}_6^-$. These data, together with elemental analysis results, support the compound's formulation as the bimetallic CO_2 -bridged dication *cis,cis*-(CH_3CN)(CO)(tpy) $\text{Ru}(\text{CO}_2)\text{Ru}(\text{tpy})(\text{CO})^{2+}2\text{PF}_6^-$ (**3**), where CO_2 is bound between the two metal centers in a $\mu_2\text{-}\eta^2$ fashion and the acetonitrile ligand is *trans* to the carboxyl ligand. The product yield for **3** was 77%. Results of experiments conducted under laboratory light were the same as those from an experiment conducted in the dark.

Treatment of an acetonitrile solution of **1** with excess aqueous sodium formate resulted in nearly quantitative conversion to a salmon-colored solid which has been characterized by spectral data and elemental analyses. The ^1H NMR spectrum revealed a pattern nearly identical with that of **1** except for the addition of a singlet at δ 7.70, which is assigned to the formate proton (see Experimental Section). The ^{13}C NMR spectrum showed two low-field resonances, at δ 195.61 and 190.68, as expected for a compound with *cis* terminal carbonyl ligands. The lower field resonance is within 1 ppm of the lowest field resonance for compound **1**; the next lowest field resonance differs from that in **1** by ca. 3 ppm. Since the carbonyl *trans* to formate (or Cl) would be affected most by ligand substitution, the lowest field resonance is assigned to the carbonyl *trans* to the central terpyridyl nitrogen; the next lowest field resonance is assigned to the carbonyl *trans* to the formate ligand. The peak at δ 167.89 is assigned to the formate carbon, and there are 8 resonances for the remaining 15 carbons in the region between δ 158.74 and 125.33. DRIFTS data showed ν_{CO} bands at 2066 and 2004 cm^{-1} and ν_{OCO} signals at 1618 and 1291 cm^{-1} , the latter being very similar to the ν_{OCO} values for *cis*- $\text{Ru}(\text{bpy})_2(\text{CO})(\text{OCHO})^+\text{PF}_6^-$ (1621 and 1282 cm^{-1}).⁸ All of the data support the formulation of the new product as the η^1 -formato complex *cis*- $\text{Ru}(\text{tpy})(\text{CO})_2(\text{OCHO})^+\text{PF}_6^-$ (**4**); the product yield was 91%. In the same manner as the

reaction of **1** with base, treatment of complex **4** with aqueous Na_2CO_3 in CH_3CN also provides the CO_2 -bridged complex **3**, again in 77% yield. Also, **4** is readily converted back to **1** by brief treatment with a catalytic amount of NaOCHO and excess tetraethylammonium chloride in aqueous CH_3CN .

The CO_2 -bridged compound **3** is sparingly soluble in CH_2Cl_2 , which allowed us to explore the possibility of displacing CH_3CN with another ligand without competition from a coordinating solvent. When **3** was slurried in CH_2Cl_2 and stirred for 30 min while CO was bubbled into the mixture, the color of the solid component of the reaction mixture changed from red to brown. Addition of ether precipitated the remainder of a brown, light-sensitive solid, which has been characterized by spectral data (the compound is stable in acetone for a short time) and elemental analysis. The ^1H NMR data showed a series of multiplets between δ 8.49 and 7.17 for the terpyridyl protons; the pattern is very similar to that for **3**. The ^{13}C NMR data showed five low-field peaks at δ 199.64, 197.57, 195.34, 190.38, and 186.28 for four terminal carbonyls and a carboxyl carbon. There are 16 resonances for the 30 remaining carbons at δ 157.90–122.26. DRIFTS data show ν_{CO} signals at 2071, 2054, 2016 and 1992 cm^{-1} and ν_{OCO} bands at 1533 and 1198 cm^{-1} ; the ν_{OCO} values for the carboxylate bridge are indicative of a $\mu_2\text{-}\eta^2$ bonding mode⁶ and are in good agreement with those observed for **3** and **2**.⁵ These data support the formulation of this compound as *cis,cis*-(CO) $_2$ (tpy) $\text{Ru}(\text{CO}_2)\text{Ru}(\text{tpy})(\text{CO})^{2+}2\text{PF}_6^-$ (**5**), where CH_3CN in **3** has been replaced by CO. As expected, when **5** was allowed to stand in acetonitrile, it reverted to **3**.

Addition of aqueous Na_2CO_3 to a solution containing equimolar amounts of **1** and $\text{Ru}(\text{bpy})_2(\text{CO})(\text{COOH})^+\text{PF}_6^-$ (**6**)⁹ in acetonitrile gave a mixture which, after analysis of the NMR spectral data, showed approximately equal amounts of **3**, unreacted acid **6** and a new product which has been characterized by spectral data, elemental analysis, and X-ray structure determination (see below). The ^1H NMR spectrum for the new product showed one low-field resonance at δ 9.48 and a series of multiplets between δ 8.60 and 6.72, which are assigned to the bipyridyl and terpyridyl protons. The ^{13}C NMR spectrum showed 4 low-field signals at δ 202.72, 202.48, 198.73, and 190.36, which have been assigned to three terminal carbonyls and a carboxylate carbon, and 35 resonances for the 35 inequivalent carbons in the region between δ 158.28 and 122.91 of the bipyridyl and terpyridyl ligands. DRIFTS data showed ν_{CO} signals at 2059, 2000 and 1940 cm^{-1} and ν_{OCO} bands at 1497 and 1186 or 1174 cm^{-1} . Again, the stretching frequencies for the carboxylate ligand are very similar to those for **2**, **3**, and **5**. These data support the formulation of the new compound as the CO_2 -bridged complex *cis,cis*-(CO)(bpy) $_2\text{Ru}(\text{CO}_2)\text{Ru}(\text{tpy})(\text{CO})^{2+}2\text{PF}_6^-$ (**7**) with the CO_2 ligand again bound in a $\mu_2\text{-}\eta^2$ fashion. The yield of **7** was maximized by slow addition of a solution of **1** in acetonitrile to a mixture containing acid **6**, CH_3CN , water, and Na_2CO_3 ; the yield was 68% by this method. Small amounts of **6** and **3** were also evident in the reaction mixture. Compound **7** has been structurally characterized (see discussion below).

(5) Gibson, D. H.; Ding, Y.; Sleadd, B. A.; Franco, J. O.; Richardson, J. F.; Mashuta, M. S. *J. Am. Chem. Soc.* **1996**, *118*, 11984.

(6) Gibson, D. H. *Chem. Rev.* **1996**, *96*, 2063.

(7) Black, D. St.-C.; Deacon, G. B.; Thomas, N. C. *Aust. J. Chem.* **1982**, *35*, 2445.

(8) Sullivan, B. P.; Caspar, J. V.; Johnson, S. R.; Meyer, T. J. *Organometallics* **1984**, *3*, 1241.

(9) Toyohara, K.; Nagao, H.; Adachi, T.; Voshida, T.; Tanaka, K. *Chem. Lett.* **1996**, 27.

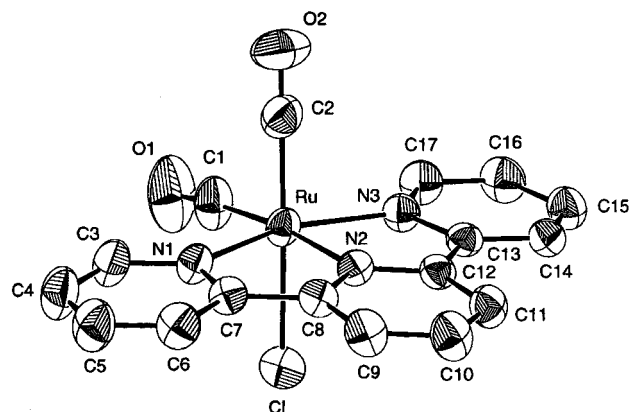


Figure 1. ORTEP diagram of **1a** (cation only) with thermal ellipsoids shown at the 50% probability level.

Table 1. Summary of Crystallographic Data for **1a** and **7**

	1a	7
formula	C ₄₁ H ₃₁ BClN ₃ O ₂ Ru	C _{40.5} H ₃₀ F ₁₂ N _{7.75} O ₅ P ₂ Ru ₂
cryst syst	triclinic	triclinic
space group	<i>P</i> 1	<i>P</i> 1
<i>a</i> , Å	13.233(4)	14.362(4)
<i>b</i> , Å	13.374(6)	14.596(3)
<i>c</i> , Å	10.918(3)	12.895(4)
α , deg	113.00(3)	93.54(2)
β , deg	98.96(2)	114.80(2)
γ , deg	78.97(3)	71.69(2)
<i>V</i> , Å ³	1738(1)	2321(1)
<i>Z</i>	2	2
<i>D_c</i> , g/cm ³	1.423	1.712
cryst dims, mm	0.60 × 0.30 × 0.26	0.60 × 0.49 × 0.49
cryst descriptn	yellow prism	orange block
μ (Mo K α), cm ⁻¹	5.68	8.20
abs cor	ψ scans	difabs
transmissn factors: min/max	0.967/1.000	0.539/1.000
radiation (λ , Å)	Mo K α (0.710 73)	
diffractometer	Enraf-Nonius CAD4	
monochromator	graphite cryst	
temp, °C	23(3)	
scan range	0.80 + 0.35 tan θ	0.85 + 0.35 tan θ
scan speed, deg/min	1–5	1–5
max 2 θ , deg	50.0	50.0
no. of unique rflns collected	6079	8139
no. of rflns included (<i>I_o</i> > 3 σ (<i>I_o</i>))	5571	6973
no. of params	443	636
computer hardware	Silicon Graphics Iris Indigo	
computer software	teXsan (msc)	
extinctn coeff	[7.30(4)] × 10 ⁻⁷	[5.29(4)] × 10 ⁻⁷
agreement factors ^a		
<i>R</i>	0.027	0.040
<i>R_w</i>	0.034	0.054
function minimized	$\sum w(F_o - F_c)^2$	
GOF	2.93	2.95
Δ/σ	0.02	0.01
weighting scheme	[$\sigma^2(F_o)$] ⁻¹	
high peak in final diff map, e/Å ³	0.39	0.50

$$^a R = \sum ||F_o| - |F_c|| / \sum (|F_o|); R_w = [\sum w(|F_o| - |F_c|)^2 / \sum w F_o^2]^{1/2}.$$

Structural Characterization of 1a and 7. The solid-state structures of **1a** and **7** were established by X-ray crystallography. The ORTEP diagram for **1a** is shown in Figure 1; crystallographic data are summarized in Table 1. Selected bond lengths and angles for **1a** are shown in Table 2. Compound **1a** exhibits slightly distorted octahedral geometry about the metal center, with cis terminal carbonyl ligands; the two carbonyls and the chloride ligand comprise a meridional plane which bisects the terpyridyl ligand. The bite angle available for a terdentate terpyridyl ligand pre-

Table 2. Selected Bond Distances (Å) and Angles (deg) for **1a**

Bond Distances			
Ru–Cl	2.3917(7)	Ru–C(1)	1.912(3)
Ru–N(1)	2.092(2)	Ru–C(2)	1.873(3)
Ru–N(2)	2.016(2)	O(1)–C(1)	1.122(3)
Ru–N(3)	2.097(2)	O(2)–C(2)	1.126(3)
Bond Angles			
Cl–Ru–N(1)	86.97(6)	N(1)–Ru–C(2)	93.1(1)
Cl–Ru–N(2)	86.21(5)	N(2)–Ru–N(3)	78.31(7)
Cl–Ru–N(3)	88.77(5)	N(2)–Ru–C(1)	172.6(1)
Cl–Ru–C(1)	86.4(1)	N(2)–Ru–C(2)	95.4(1)
Cl–Ru–C(2)	178.39(9)	N(3)–Ru–C(1)	102.30(9)
N(1)–Ru–N(2)	79.01(7)	N(3)–Ru–C(2)	91.8(1)
N(1)–Ru–N(3)	157.14(7)	C(1)–Ru–C(2)	92.0(1)
N(1)–Ru–C(1)	99.8(1)	Ru–C(1)–O(1)	175.8(3)
Ru–C(2)–O(2)	178.3(3)		

vents it from participating in idealized octahedral geometry. As a consequence, the N(1)–Ru–N(3) bond angle is 157.14(7)°, with the Ru–N(1) and Ru–N(3) bond lengths slightly elongated (2.092(2) and 2.097(2) Å, respectively) relative to Ru–N bonds in less constrained bipyridyl complexes (in Ru(bpy)₂Cl₂¹⁰ and Ru(bpy)₂(CO)(COOH)⁺O₃SCF₃^{–9} the average Ru–N bond which is trans to a bpy nitrogen is 2.054 Å in length). The Ru–N(2) bond (involving the central terpyridyl nitrogen) in **1a** is compressed at 2.016(2) Å; the Ru–Cl bond length is 2.391(7) Å. More closely related to **1a** is the neutral complex *cis*-Ru(tpy)(CO)Cl₂, which has been structurally characterized by Deacon et al.¹¹ Here, the Ru–Cl bond is longer when this ligand is trans to CO (2.438(3) Å) than when the relationship is *cis* (2.420(3) Å). Again, the Ru–N bond of the central nitrogen in the tpy ligand is shorter (1.969(7) Å as compared to approximately 2.08 Å for the other two). The Ru–C(2) bond in **1a** (trans to Cl) is somewhat shorter, at 1.873(3) Å, than that of Ru–C(1) (trans to tpy), at 1.912(3) Å. The Ru–Cl bond distance (2.3917(7) Å) is very similar to that in *cis*-Ru(bpy)₂(CO)(Cl)⁺ (2.396(7) Å),¹² even though a *cis* relationship of the chloride and carbonyl ligands exists in this cation. Compound **1a** is cationic; the reduced electron density about the ruthenium atom in **1a** may be responsible for the contraction of the Ru–Cl bond (which is trans to CO in this compound) relative to the analogous Ru–Cl bond in *cis*-Ru(tpy)(CO)Cl₂.

The ORTEP diagram for the CO₂-bridged complex **7** is shown in Figure 2 and clearly shows a μ_2 - η^2 -bound CO₂ ligand; crystallographic data are shown in Table 1, and selected bond distances and angles are given in Table 3. Compound **7** exhibits slightly distorted octahedral geometry about both metal centers. Bond angles and distances for the tpy-containing portion of the molecule do not deviate significantly from those in **1a**. The bpy-containing portion of the molecule displays bond lengths and angles which are similar to those reported by Tanaka et al.¹³ for the metalloester Ru(bpy)₂(CO)(C(O)OMe)⁺PF₆[–]. The only other structurally characterized, and non-metallacyclic, complex with

(10) Eggleston, D. S.; Goldsby, K. A.; Hodgson, D. J.; Meyer, T. J. *Inorg. Chem.* **1985**, *24*, 4573.

(11) Deacon, G. B.; Patrick, J. M.; Skelton, B. W.; Thomas, N. C.; White, A. H. *Aust. J. Chem.* **1984**, *37*, 929.

(12) Clear, J. M.; Kelly, J. M.; O'Connell, C. M.; Vos, J. G.; Cardin, C. J.; Costa, S. R.; Edwards, A. J. *J. Chem. Soc., Chem. Commun.* **1980**, 750.

(13) Tanaka, H.; Tzeng, B.-C.; Nagao, H.; Peng, S.-M.; Tanaka, K. *Inorg. Chem.* **1993**, *32*, 1508.

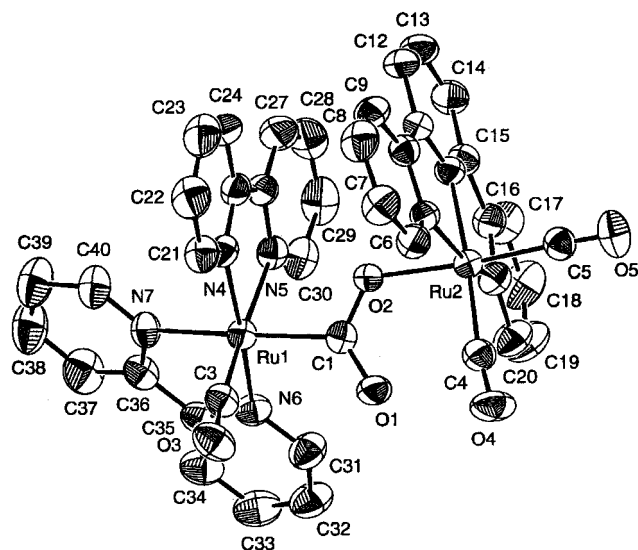


Figure 2. ORTEP drawing of **7** (cation only) with thermal ellipsoids shown at the 50% probability level.

Table 3. Selected Bond Distances (Å) and Angles (deg) for **7**

Bond Distances			
Ru(1)–N(4)	2.060(3)	Ru(2)–N(1)	2.078(3)
Ru(1)–N(5)	2.116(3)	Ru(2)–N(2)	2.014(3)
Ru(1)–N(6)	2.099(3)	Ru(2)–N(3)	2.087(3)
Ru(1)–N(7)	2.183(3)	Ru(2)–C(4)	1.921(5)
Ru(1)–C(1)	2.059(4)	Ru(2)–C(5)	1.886(4)
Ru(1)–C(3)	1.835(5)	O(1)–C(1)	1.232(4)
Ru(2)–O(2)	2.058(3)	O(2)–C(1)	1.297(5)
O(3)–C(3)	1.151(5)	O(4)–C(4)	1.132(5)
O(5)–C(5)	1.118(5)		
Bond Angles			
N(4)–Ru(1)–C(1)	89.3(1)	O(2)–Ru(2)–N(2)	80.7(1)
N(4)–Ru(1)–C(3)	96.8(2)	O(2)–Ru(2)–N(3)	86.8(1)
N(5)–Ru(1)–C(1)	88.3(1)	O(2)–Ru(2)–C(4)	95.3(1)
N(5)–Ru(1)–C(3)	172.9(1)	O(2)–Ru(2)–C(5)	175.6(1)
N(6)–Ru(1)–C(1)	97.5(1)	N(1)–Ru(2)–C(4)	101.1(2)
N(6)–Ru(1)–C(3)	91.0(2)	N(1)–Ru(2)–C(5)	92.6(2)
N(7)–Ru(1)–C(1)	171.1(1)	N(2)–Ru(2)–C(4)	176.0(1)
N(7)–Ru(1)–C(3)	100.3(2)	Ru(1)–C(1)–O(1)	124.6(3)
C(1)–Ru(1)–C(3)	86.6(2)	Ru(1)–C(1)–O(2)	114.1(3)
O(2)–Ru(2)–N(1)	84.3(1)	O(1)–C(1)–O(2)	121.3(4)
Ru(1)–C(3)–O(3)	175.9(4)	Ru(2)–O(2)–C(1)	123.1(2)
Ru(2)–C(5)–O(5)	177.2(4)	Ru(2)–C(4)–O(4)	172.5(4)

$\mu_2\text{-}\eta^2$ binding of CO_2 between two transition metals, $\text{Cp}(\text{CO})(\text{PPh}_3)\text{Fe}(\text{CO})_2\text{Re}(\text{CO})_4(\text{PPh}_3)$ ($\text{Cp} = \eta^5\text{-cyclopentadienyl}$),¹⁴ has angles and distances involving the CO_2 bridge ($\text{C}(1)\text{--O}(1) = 1.226(3)$ Å; $\text{C}(1)\text{--O}(2) = 1.298(3)$ Å; $\text{O}\text{--C}\text{--O} = 121.9(3)^\circ$) which are very similar to those in **7** (see Table 3). Finally, the ruthenium–nitrogen bond which is trans to the carboxyl carbon is unusually long, at 2.183(3) Å; only $\text{Ru}(\text{bpy})_2(\text{CO})(\text{CO}_2)\cdot 3\text{H}_2\text{O}$ displays a longer corresponding bond in the ruthenium bipyridyl series of compounds, at 2.204(10) Å.¹²

Considerations of Reaction Paths. Efforts to remove the chloride ligand from **1** with silver or thallium salts, or by thermal displacement with an acetonitrile ligand, were unsuccessful. The labilization of the Ru–Cl bond which occurs with **1** in the presence of aqueous base appears to occur indirectly, as the result of changes at the terminal carbonyl ligand trans to chlorine. Recently, Pakkanen and co-workers¹⁵ have structurally characterized $\text{cis}(\text{CO})\text{-Ru}(\text{bpy})(\text{CO})_2(\text{C}(\text{O})\text{OMe})\text{Cl}$; it is one of the few transition metal complexes having a chloride ligand trans to an acyl group in an octahedral complex for which structural data are available. This compound displays an even longer Ru–Cl bond (2.496(3) Å) than the closely related dichloro dicarbonyl complex $\text{cis},\text{cis}\text{-Ru}(\text{bpy})(\text{CO})_2\text{Cl}_2$ (2.439(3) Å).¹⁵ The lengthening of the Ru–Cl bond in the metalloester has been attributed to the trans effect of the σ -donating acyl ligand, an effect well documented in square-planar complexes.¹⁶ A long Ru–Cl bond is present in $\text{cis}(\text{CO})\text{-Ru}(\text{bpy})(\text{CO})_2(\text{C}(\text{O})\text{OMe})\text{Cl}$, even though the complex has two terminal carbonyl ligands which can help to dissipate the additional electron density on the metal center via back-bonding. Nucleophilic addition to the terminal carbonyl in **1** which is trans to Cl would leave a species with only one terminal carbonyl ligand, thus setting the stage for complete dissociation of the chloride ligand.

The proposed pathways for the formation of the formate complex (**4**) and CO_2 -bridged complex **3** from **1** are given in Scheme 1. The suggested initial step for both transformations is nucleophilic addition of hydroxide ion to the carbonyl ligand which is trans to chlorine, resulting in intermediate **A**. Conversion of the π -acceptor CO to the σ -donating acyl group of the metalcarboxylic acid results in labilization of Cl^- and initial formation of a five-coordinate metalcarboxylic acid intermediate, **B** (which may be quickly solvated). In the reaction with aqueous NaOCHO , coordination of formate ion (which is present in excess) at the position trans to the carboxyl group in **B** would result in hydroxide dissociation and generation of **4**. Under the more basic conditions provided by aqueous Na_2CO_3 , nucleophilic attack of a carboxylate oxygen from **B** (as with other $\text{M}\text{--COOH}$, not deprotonated by this base) at the position trans to COOH in a second **B** molecule (or solvated **B**) would promote hydroxide dissociation from the carboxyl group of the second molecule, in the manner of the formate reaction. Deprotonation of the carboxyl bridge and coordination of CH_3CN would provide the CO_2 -bridged complex **3**.

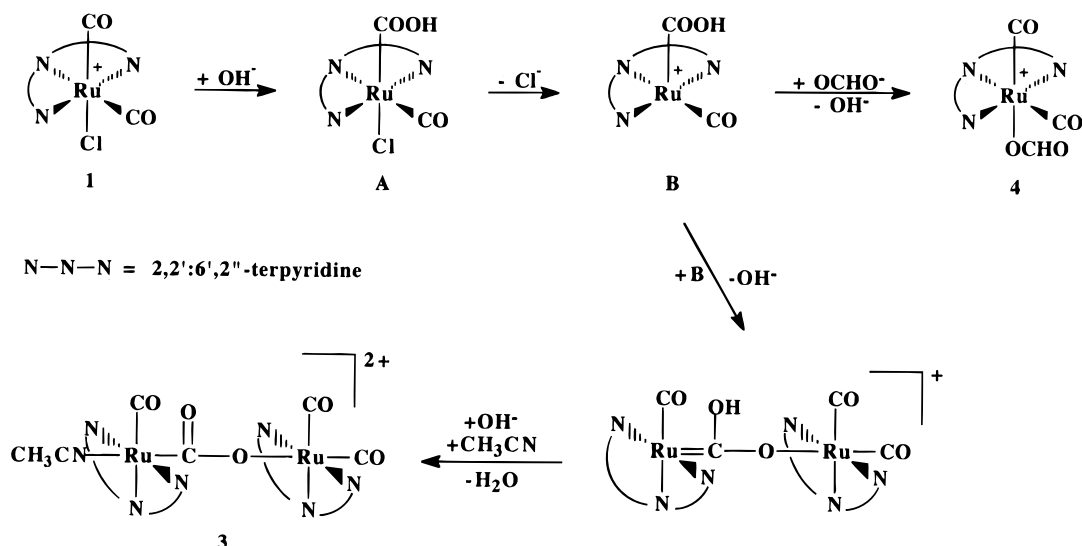
The lability of the formate ligand in **4** toward dissociation is evidenced by the ease of conversion of **4** back to **1** by reaction with Cl^- . Thus, the ease with which **4** can be converted to the CO_2 -bridged compound **3** by the action of aqueous sodium carbonate is not surprising. Several observations on the lability of the position trans to the acyl carbon in **3** and **5** are worthy of note. Compound **3** exhibits good solubility only in acetone or CH_3CN ; however, dissolution of this compound in acetone is followed by rapid decomposition to many unidentifiable products. Attempts to return chloride to that position, using excess Et_4NCl in CH_3CN solution in the manner in which **4** can be converted back to **1**, were unsuccessful and resulted in decomposition of **3**. For compound **5** in the solid state, decomposition occurs after several hours under laboratory lights, presumably via loss of CO. Furthermore, dissolution of **5** in CH_3CN

(15) Haukka, M.; Kiviaho, J.; Ahlgren, M.; Pakkanen, T. A. *Organometallics* **1995**, *14*, 825.

(16) See, for example: (a) Weaver, D. L. S. *Inorg. Chem.* **1970**, *9*, 2250. (b) Appleton, T. G.; Clark, H. C.; Manzer, L. E. *Coord. Chem. Rev.* **1973**, *10*, 335. (c) Bennett, M. A.; Johnson, R. N.; Robertson, G. B.; Tomkins, I. B.; Whimp, P. O. *J. Am. Chem. Soc.* **1976**, *98*, 3514. (d) Anderson, O. P.; Packard, A. B. *Inorg. Chem.* **1978**, *17*, 1333. (e) Bardi, R.; Piazzesi, A. M.; Del Pra, A.; Cavinato, G.; Toniolo, L. *Inorg. Chim. Acta* **1985**, *102*, 99.

(14) Gibson, D. H.; Ye, M.; Richardson, J. F. *J. Am. Chem. Soc.* **1992**, *114*, 9716.

Scheme 1



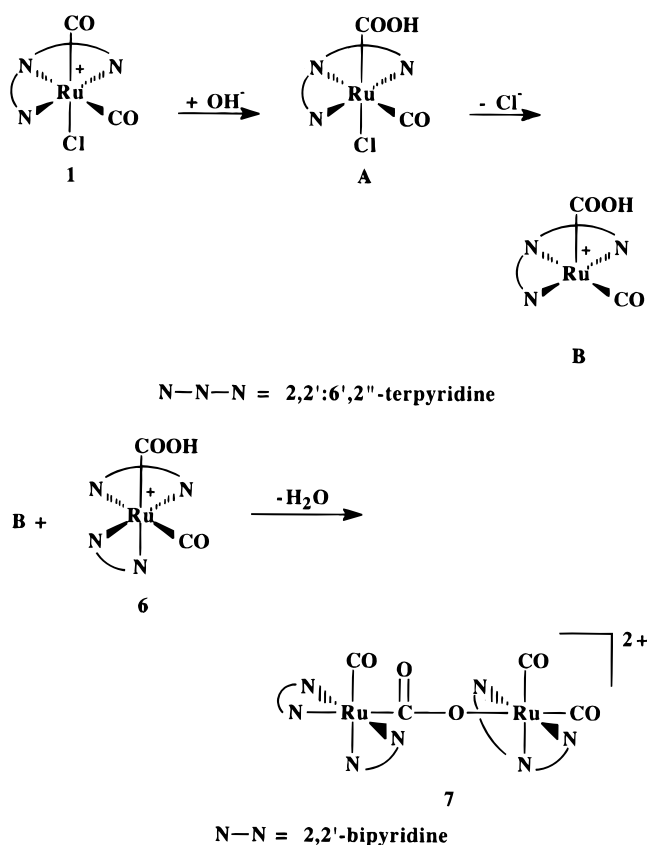
results in immediate loss of CO and conversion to **3**, as noted above.

Since formation of **3** from the reaction of **1** or **4** with aqueous Na₂CO₃ suggested the possible intermediacy of a metallocarboxylic acid, we decided to probe the reactions of **1** further in the presence of a metallocarboxylic acid. The known¹⁷ acid *cis*-Ru(bpy)₂(CO)-(COOH)⁺PF₆[−] (**6**), which can be prepared by the reaction of *cis*-Ru(bpy)₂(CO)₂²⁺(2PF₆[−])₂ with aqueous Na₂CO₃,⁵ does not react further with this base. These properties suggested its use as a potential trapping agent for intermediate **B** in the reactions of **1** or **4** with aqueous Na₂CO₃, thus providing support for this proposed active species in the formation of the CO₂-bridged compound **3**. Initially, the yield of **7** from reaction between **1** and **6** was relatively low. The nucleophilicity of intermediate **B** is apparently comparable to that of **6**, since only half of **6** was consumed when this compound and **1** were present in solution prior to the addition of base. The problem was reduced, and the yield of **7** was enhanced, by putting **6** and the aqueous base together before adding compound **1**. The proposed rationale for the formation of **7** is shown in Scheme 2. The unsymmetrical nature of **7** eliminated the potential for crystallographically imposed disorder in the carboxylate bridge, a problem which hindered structural refinement of *cis,cis*-(CO)(bpy)₂Ru(CO₂)Ru(bpy)₂(CO)₂²⁺2PF₆[−] (**2**).⁵

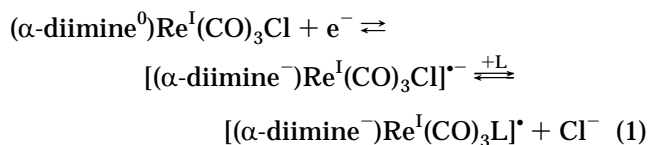
In 1983, Hawecker, Lehn, and Ziessel^{1d} reported the use of *fac*-Re(bpy)(CO)₃Cl as a catalyst for the photoinduced reduction of CO₂ and noted that halide dissociation occurred. These observations were followed by additional studies from this group and from Meyer and Sullivan et al.^{1c,f,g} noting the generality of such reactions. The latter group also reported that two sequential one-electron reductions of [M(bpy)₂(L)Cl]ⁿ⁺ (M = Ru, Os; L = Cl, pyridine, PR₃, CO) in CH₃CN resulted in facile dissociation of Cl[−] and replacement by CH₃CN.^{1c} This group also noted that the formate ligand in Ru(bpy)₂(CO)(OCHO)⁺PF₆[−] was labilized under similar electrochemical conditions.

The mechanisms by which these ligand labilizations occur, and their role in CO₂ reduction, have been the

Scheme 2



subject of numerous studies and remain an active area of investigation.^{11–m} The electron transfer step in complexes involving α -diimine ligands coordinated to Ru and Re centers has been regarded as a reduction of the diimine ligand followed by halide dissociation from the metal, as shown in eq 1. However, recent *in situ* FTIR

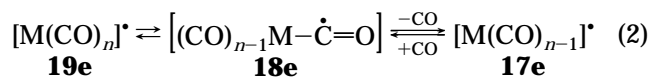


studies of the electrocatalyzed reductions of CO₂ by *fac*-

(17) Ishida, H.; Tanaka, K.; Morimoto, M.; Tanaka, T. *Organometallics* **1986**, 5, 724.

Re(bpy)(CO)₃Cl have provided some clarification and IR spectral data on intermediate reduced species.^{1k,l} The starting material shows IR bands (in CH₃CN) for the terminal carbonyls at 2020, 1914 and 1897 cm⁻¹; after reduction to the radical anion, the bands are lowered to 1998, 1885, and 1867 cm⁻¹. The lowering of these stretching frequencies clearly demonstrates that the increased electron density is being shared by the carbonyl ligands even though the bipyridyl ligand may bear most of it. Kaim et al.^{1m} have described the dissociation of halide as resulting from overlap of the π* orbital of the diimine with the σ(Re–Hal) antibonding orbital as well as ligand to metal electron transfer which determines the extent of activation; the diimine ligand is proposed to serve as an “electron buffer”.

With many other metal carbonyl complexes, electron transfer to the compounds has been shown to yield 19e species which establish equilibrium with 18e metal acyl radicals.¹⁸ Ligand dissociation can follow this conversion, resulting in a 17e coordinatively unsaturated metal radical, as shown in eq 2. In several cases, however,



the 18e acyl radical has been intercepted by H-atom abstraction and conversion to a formyl complex.

We suggest that metal acyl radicals, present in small concentrations, play an active role in the halide labilizations which occur under photochemical and electrochemical reactions with the diimine complexes. As in our nucleophilic additions to compound **1**, the driving force for halide loss in these reactions is suggested to be due, in part, to the conversion of a terminal carbonyl ligand (π-acceptor) to a σ-donor acyl ligand.

Experimental Section

General data. Reagent grade solvents dichloromethane, diethyl ether, ethanol, acetone and acetonitrile were used as received. Acetone-*d*₆ and CD₃CN were obtained from Cambridge Isotope Laboratories. RuCl₃·nH₂O was purchased from Pressure Chemical Co., and 2,2':6',2''-terpyridyl (tpy) was purchased from Aldrich or Strem Chemicals, Inc.; Et₄NCl (monohydrate), TIPF₆, and AgBF₄ were obtained from Aldrich. [Ru(CO)₂Cl₂]_n² and *cis*-Ru(bpy)₂(CO)(COOH)⁺PF₆⁻¹⁷ were prepared as described previously. Spectral data were obtained on the following instruments: NMR, Bruker AMX-500; FTIR, Mattson RS1. Diffuse-reflectance FTIR data were obtained on the Mattson instrument with a DRIFTS accessory (Graseby Specac Inc., “Mini-Diff”) as KCl dispersions.¹⁹ ¹H and ¹³C NMR chemical shifts were referenced to residual protons in the deuterated solvents. Melting points were obtained on a Thomas-Hoover capillary melting point apparatus and are uncorrected. Elemental analyses were performed by Midwest Microlab, Indianapolis, IN.

***cis*-Ru(tpy)(CO)₂Cl⁺PF₆⁻ (1).** (a) A 1.0 g (4.4 mmol) amount of [Ru(CO)₂Cl₂]_n and 1.1 g (4.7 mmol) of 2,2':6',2''-terpyridine were introduced into a flask containing ca. 60 mL of H₂O/EtOH (1:1, v:v) and the mixture was refluxed for 3 h.

(18) See: (a) Narayanan, B. A.; Kochi, J. K. *Organometallics* **1986**, 5, 926. (b) Wayland, B. B.; Sherry, A. E.; Coffin, V. L. In *Homogeneous Transition Metal Catalyzed Reactions*; Moser, W. R., Slocum, D. W., Eds.; Adv. Chem. Ser. 230; American Chemical Society: Washington, DC, 1992; Chapter 17. (c) Astruc, D. *Electron Transfer and Radical Processes in Transition Metal Chemistry*; VCH: New York, 1995; Chapters 5 and 6, and references cited therein.

(19) Griffiths, P. W.; deHaseth, J. A. *Fourier Transform Infrared Spectroscopy*; Wiley: New York, 1986; Chapter 5.

The clear yellow solution was cooled to room temperature, and 1.0 g (6.1 mmol) of NH₄PF₆ dissolved in a minimum amount of water was added, followed by ca. 50 mL of water. The resulting precipitate was collected by filtration and recrystallized from CH₃CN/ether to give 1.6 g (80% yield based on Ru(CO)₂Cl₂ monomer) of a cream-colored solid, mp >240 °C.

Anal. Calcd for C₁₇H₁₁ClF₆N₃O₂PRu: C, 35.77; H, 1.94. Found: C, 35.87; H, 2.04. IR (DRIFTS, KCl): ν_{CO} 2092 and 2029 cm⁻¹. ¹H NMR (CD₃CN): δ 8.75 (d, *J*_{HH} = 5.5 Hz), 8.49–7.67 (m). ¹³C NMR (CD₃CN): δ 194.94, 187.31, 158.08–125.29 (8 resonances for 15 carbons).

(b) The tetraphenylborate salt of this cation (**1a**) was prepared as above, using aqueous NaBPh₄ as the anion exchange reagent. Spectral data were in good agreement with the above values, with the addition of three multiplets at 7.28, 6.98, and 6.81 ppm (integral ratio 2:2:1) for the tetraphenylborate anion.

Attempted Removal of Chloride from 1. (a) Under N₂, 0.10 g (0.17 mmol) of **1** and 0.70 g (0.20 mmol) of TIPF₆ were dissolved in ca. 30 mL of dry acetonitrile and this solution was refluxed for 24 h. IR spectral data obtained during this time showed no evidence of reaction. Solvent was then removed under vacuum, and the residue was analyzed by NMR spectroscopy; the spectral data showed no evidence for conversion of **1**.

(b) Similarly, 0.10 g of **1** and 0.04 g (0.20 mmol) of AgBF₄ were placed in 30 mL of dry acetonitrile and the mixture was refluxed for 24 h. Again, spectral data obtained during this time, or after the reaction period, showed no evidence for conversion of **1**.

(c) Compound **1** 0.10 g, 0.17 mmol) was dissolved in 20 mL of acetonitrile and the solution was refluxed for 3 days. The solution was concentrated to a small volume and then concentrated aqueous NH₄PF₆ was added (to effect anion exchange if needed). The ¹H NMR spectrum of the crude product showed only unreacted **1**.

***cis,cis*-(CH₃CN)(CO)(tpy)Ru(CO₂)Ru(tpy)(CO)₂²⁺-2PF₆⁻ (3).** (a) A 0.30 g (0.53 mmol) amount of **1** was dissolved in ca. 30 mL of CH₃CN, and 1 mL of saturated aqueous Na₂CO₃ was added. The mixture was stirred for 2 h, and the solvent was removed under vacuum. The residue was extracted with CH₃CN and filtered. Ether was added to the filtrate to effect the precipitation of 0.23 g (77% yield) of a deep red solid, mp >240 °C. Although this experiment was conducted under laboratory lights, a similar experiment conducted in the dark gave the same results after the same time.

Anal. Calcd for C₃₆H₂₅F₁₂N₇O₅P₂Ru₂: C, 38.34; H, 2.23. Found: C, 38.42; H, 2.36. IR (DRIFTS, KCl): ν_{CO} 2069, 2013, and 1953 cm⁻¹; ν_{OCO} 1503 and 1177 cm⁻¹; ν_{CN} 2313 and 2283 cm⁻¹. ¹H NMR (CD₃CN): δ 8.49 (t, *J*_{HH} = 8.0 Hz), 8.37–7.17 (m). ¹³C NMR (CD₃CN): δ 204.25, 198.23, 195.38, 190.18, 157.90–122.26 (16 resonances for 30 carbons).

(b) A 0.20 g (0.34 mmol) amount of **4** was dissolved in ca. 30 mL of CH₃CN, and 1 mL of saturated aqueous Na₂CO₃ was added. The mixture was stirred for 1.5 h, and the solvent was removed under vacuum. The residue was extracted with CH₃CN and the extract filtered. Ether was added to the filtrate to effect the precipitation of 0.15 g (77% yield) of a deep red solid whose spectral properties were identical with those of **3**.

***cis*-Ru(tpy)(CO)₂(OCHO)⁺PF₆⁻ (4).** 0.10 g (0.18 mmol) amount of **1** was dissolved in ca. 20 mL of CH₃CN, and 1 mL of saturated aqueous Na(OCHO) was added. The mixture was stirred for 1 h, and the solvent was removed under vacuum. The residue was extracted with CH₃CN and filtered. Ether was added to the filtrate to effect precipitation of 0.09 g (91% yield) of a salmon-colored solid, mp 210 °C dec.

Anal. Calcd for C₁₈H₁₂F₆N₃O₄PRu: C, 37.25; H, 2.08. Found: C, 37.33; H, 2.09. IR (DRIFTS, KCl): ν_{CO} 2066 and 2004 cm⁻¹; ν_{OCO} 1618 and 1291 cm⁻¹. ¹H NMR (CD₃CN): δ 8.76 (d, *J*_{HH} = 5.0 Hz), 8.48–7.63 (m). ¹³C NMR (CD₃CN): δ 195.61, 190.68, 167.89, 158.74–125.33 (8 resonances for 15 carbons).

Conversion of 4 to 1. A 0.22 g (0.38 mmol) amount of **4** was dissolved in ca. 20 mL of acetonitrile; 0.40 g (2.41 mmol) of Et₄Cl (monohydrate) and 0.5 mL of saturated NaOCHO were added, and the solution was stirred for 5 min. The solution was then concentrated to 5 mL, and concentrated aqueous NH₄PF₆ was added to effect anion exchange. ¹H NMR analysis of the resulting precipitate showed that it consisted entirely of **1**; the isolated yield of **1** after crystallization from CH₃CN/ether was 0.17 g (78%). Also, a similar experiment conducted in the dark gave the same results. However, a similar experiment conducted without NaOCHO afforded no conversion of **4** to **1**.

cis,cis-(CO)₂(tpy)Ru(CO₂)Ru(tpy)(CO)₂²⁺2PF₆⁻ (5**).** A 0.041 g (0.036 mmol) amount of **3** was added to ca. 30 mL of CO-saturated CH₂Cl₂, and the mixture was stirred, with continuous bubbling of CO, for 1.5 h. Ether was then added to effect the precipitation of 0.033 g (83% yield) of a light brown solid, mp 165 °C dec.

Anal. Calcd for C₃₅H₂₂F₁₂N₆O₆P₂Ru₂: C, 37.71; H, 1.99. Found: C, 37.83; H, 2.09. IR (DRIFTS, KCl): ν_{CO} 2071, 2054, 2016, and 1992 cm⁻¹; ν_{OCO} 1533 and 1198 cm⁻¹. ¹H NMR (acetone-*d*₆): δ 8.71–8.66 (m), 8.55 (d, *J*_{HH} = 6.5 Hz), 8.46 (d, *J*_{HH} = 5.5 Hz), 8.33–7.44 (m). ¹³C NMR (acetone-*d*₆): δ 199.64, 197.57, 195.34, 190.38, 186.28, 158.02–123.35 (16 resonances for 30 carbons).

cis,cis-(CO)(bpy)₂Ru(CO₂)Ru(tpy)(CO)₂²⁺2PF₆⁻ (7**).** A 0.20 g (0.31 mmol) amount of *cis*-Ru(bpy)₂(CO)(COOH)⁺PF₆⁻ (**6**) was dissolved in ca. 20 mL of CH₃CN, followed by addition of 1 mL of saturated aqueous Na₂CO₃. A 0.18 g (0.31 mmol) amount of **1** was dissolved in a minimum amount of CH₃CN, and this solution was added dropwise over ca. 30 min to the vigorously stirred mixture. The reaction mixture was allowed to stir for an additional 1 h, and the solvent was removed under vacuum. The resultant residue was extracted with CH₃CN and filtered. Ether was then added to the filtrate to effect the precipitation of 0.25 g (68% yield) of a red crystalline solid, mp 210 °C (dec).

Anal. Calcd for C₃₉H₂₇F₁₂N₇O₅P₂Ru₂: C, 40.18; H, 2.33. Found: C, 40.19; H, 2.42. IR (DRIFTS, KCl): ν_{CO} 2059, 2000, and 1940 cm⁻¹; ν_{OCO} 1497 and 1186 or 1174 cm⁻¹. ¹H NMR (CD₃CN): δ 9.48 (d, *J*_{HH} = 5.5 Hz), 8.60–6.72 (m). ¹³C NMR (CD₃CN): δ 202.72, 202.48, 198.73, 190.36, 158.28–122.91 (35 inequivalent carbons).

X-ray Crystal Structure of 1a. A suitable crystal was grown by slow diffusion of ether into a CH₃CN solution of **1a**. Data were collected on an Enraf-Nonius CAD4 diffractometer at 23 °C; the crystallographic data are outlined in Table 1. Selected bond distances and bond angles are shown in Table 2. Of 6079 unique reflections, 5571 were considered observed (*I* > 3σ(*I*)). The structure was solved using direct methods

(SIR92²⁰) and refined with anisotropic thermal parameters for all non-hydrogen atoms. The calculated positions and thermal parameters for the H atoms were kept constant with temperature factors set to 1.2 times those of the carbon atoms to which they are bonded. A final *R* index of 0.027 with *R*_w = 0.034 was obtained for 433 variables. All computations were performed using the teXsan²¹ package (Molecular Structure Corp.).

X-ray Crystal Structure of 7. A suitable crystal was grown by slow diffusion of ether into a CH₃CN solution of **7**. Data were collected on an Enraf-Nonius CAD4 diffractometer at 23 °C; the crystallographic data are outlined in Table 1. Selected bond distances and bond angles are shown in Table 3. Of 8139 unique reflections, 6976 were considered observed (*I* > 3σ(*I*)). The structure was solved using direct methods (SIR92²⁰) and refined with anisotropic thermal parameters for all non-hydrogen atoms except for one disordered PF₆ anion; the structure included a partial (3/4) occupancy CH₃CN solvate molecule. The PF₆ disorder (rotational) was modeled using 3/4 occupancy for four fluorine atoms which were refined anisotropically and completed using a second set of four 1/4 occupancy fluorine atoms that were refined isotropically. The calculated positions and thermal parameters for the H atoms were kept constant with temperature factors set to 1.2 times those of the carbon atoms to which they are bonded. A final *R* index of 0.040 with *R*_w = 0.054 was obtained for 636 variables. All computations were performed using the teXsan²¹ package (Molecular Structure Corp.).

Acknowledgment. Support of this work by the United States Department of Energy, Division of Chemical Sciences (Office of Basic Energy Sciences), Office of Energy Research, is gratefully acknowledged. The X-ray equipment was purchased with assistance from the National Science Foundation (Grant No. CHE-9016978). Fellowship support to B.A.S. from the United States Department of Education through a GAANN grant is also gratefully acknowledged.

Supporting Information Available: Tables of crystallographic data, positional and isotropic thermal parameters, anisotropic thermal parameters, H atom positional parameters, bond distances, and bond angles for **1a** and **7** (29 pages). Ordering information is given on any current masthead page.

OM970493P

(20) Altomare, A.; Cascarano, G.; Giacovazzo, C.; Guagliardi, A.; Burla, M. C.; Polidori, G.; Camalli, M. *J. Appl. Crystallogr.* **1994**, *27*, 435.

(21) teXsan: Single Crystal Structure Analysis Software, Version 1.6 (1993); Molecular Structure Corp., The Woodlands, TX 77381.